Assignment 2

Networked and Distributed Control - SC42101

Joshua C.S. Amato (4688368)

May 30, 2024

1 (Non-)Deterministic Packet Loss

1.1 ω-automaton

Let us firstly consider system 1. By the problem formulation, system 1 may have a finite sequence of 3 consecutive packets received or a finite sequence of two consecutive packets received and one dropped. Therefore the recognized ω-language is:

$$m^1 \models ((000)^* \circ (001)^*)^\omega \tag{1.1}$$

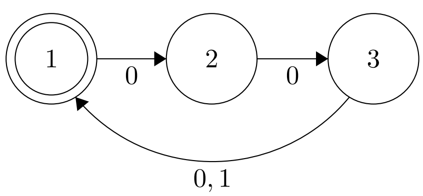

Figure 1: Visual representation of ω-automaton of system 1

In contrast, in system 2 we know that every other packet is lost. Hence $m_k = 0$ and $m_k = 1$ alternate, where for $m_k \in \{0,1\}$ $m_k = 1$ means a packet is lost at sampling index k and viceversa, assuming the first package is not lost. Therefore the recognized ω-language is :

$$m^2 \models (01)^\omega \tag{1.2}$$

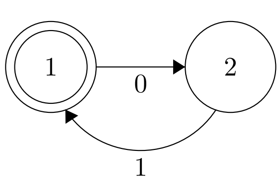

Figure 2: Visual representation of ω automaton of system 2

1.2 Dynamics of received samples

System 2 is described first as it is the simpler case. Recalling the ω-language m^2, it is clear that the switching sequence is deterministic and known. Therefore, we can define a new signal $x_l \subset \mathcal{L} \times \mathbb{R}^2$ with the tag $l \in \mathcal{L}$ of received samples, shown in figure 3.

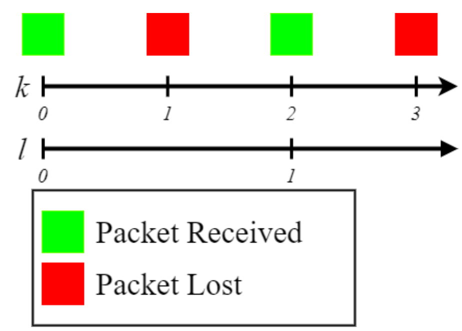

Figure 3: Comparison of tag l of received samples instead of sampling tag k

Using this newly defined signal and tag, we can define its underlying closed-loop dynamics, and convert the switched system dynamics into an LTI representation:

$$x_{l+1}^{(e)} := \tilde{\mathcal{F}}_{cl}^{i} = \mathcal{F}_1^i \mathcal{F}_0 x_l, \quad \forall l \in \mathcal{L}, i \in \{h, z\} \tag{1.3}$$

The matrices in the to-hold strategy are given by ($F_2 = e^{A_2 h_2}$):

$$x_{k+1}^e = \begin{cases} \mathcal{F}_0^h x_k := \begin{bmatrix} (F_2(h_2) - G(h_2)\bar{K}_2) & 0 \\ -\bar{K}_2 & 0 \end{bmatrix} x_k^e, m_k = 0 \\ \mathcal{F}_1^h x_k := \begin{bmatrix} F_2(h_2) & G(h_2) \\ 0 & I \end{bmatrix} x_k^e, \ m_k = 1 \end{cases} \tag{1.4}$$

whils in the to-zero strategy:

$$x_{k+1} = \begin{cases} \mathcal{F}_0^z x_k := (F_2(h_2) - G(h)\bar{K}_2)x_k, & m_k = 0 \\ \mathcal{F}_1^z x_k := F_2(h_2)x_k, & m_k = 1 \end{cases} \tag{1.5}$$

System 1 is slightly more complicated, since here we have a "second layer" of switching, introducing a non-deterministic component. Let us define, similarly to system 2, a new signal $x_\lambda \subset \Lambda \times \mathbb{R}^2$ with the tag $\lambda \in \Lambda$. Here, we "monitor" the accepting state, introducing the following closed-loop dynamics:

$$x^{(e)}_{\lambda+1} = \begin{cases} \tilde{F}^{0,i}_{cl} := F_0^i F_0^i F_0^i, \; m_\lambda = (000) \\ \tilde{F}^{1,i}_{cl} := F_0 F_0 F_1^i, \; m_\lambda = (001) \end{cases} \tag{1.6}$$

where again $i \in \{h, z\}$ and $m_\lambda = m_{k-2}m_{k-1}m_k$. The matrices in the to-hold strategy are given by:

$$x^e_{k+1} = \begin{cases} F_0^h x^e_k := \begin{bmatrix} (F(h_1) - G(h_1)\bar{K}) & 0 \\ -\bar{K} & 0 \end{bmatrix} x^e_k, \; m_k = 0 \\ F_1^h x^e_k := \begin{bmatrix} F(h_1) & G(h_1) \\ 0 & I \end{bmatrix} x^e_k, \; m_k = 1 \end{cases} \tag{1.7}$$

whilst in the to-zero strategy:

$$x_{k+1} = \begin{cases} F_0^z x_k := (F(h_1) - G(h_1)\bar{K})x_k, & m_k = 0 \\ F_1^z x_k := F(h_1)x_k, & m_k = 1 \end{cases} \tag{1.8}$$

1.3 Stability

Subsequently, we can check the stability of systems 1 and 2. Note that system 2 is an LTI dynamical system, hence it is sufficient to perform an eigenvalue check on the matrix [1] $\tilde{\mathcal{F}}^i_{cl}$. However, system 1 is a time-varying system, therefore we must us Linear Matrix Inequalities (LMIs) to guarantee stability. Therefore, we can use proposition 1 to guarantee stability of the joint networked control system.

Proposition 1 *The origins of System 1 and System 2 as described in Assignment 2.1, with their respective sequences m^1 and m^2 defined in section 1.1, are jointly (i.e., both simultaneaously) globally exponentially stable if and only if:*

$$\rho(\tilde{\mathcal{F}}^i_{cl}) < 1, \quad i \in \{h, z\}$$

and if there exist a matrix $P = P^T \succ 0$ such that the following LMI holds:

$$\begin{bmatrix} (\tilde{F}^{0,i}_{cl})^T P \tilde{F}^0_{cl} - P & 0 \\ 0 & (\tilde{F}^{1,i}_{cl})^T P \tilde{F}^0_{cl} - P \end{bmatrix} \preceq -Q$$

for some $Q = Q^T \succ 0$, given an $i \in \{h, z\}$, h_1 and $h_2 = 3h_1$.

For stability of System 2, we can also define an equivalent LMI to guarantee stability. Namely, if there exist a matrx $P = P^T \succ 0$ such that equation 1.9 holds for some $Q = Q^T$, then System 2 is globally exponentially stable:

$$(\tilde{\mathcal{F}}^i_{cl})^T P \tilde{\mathcal{F}}^i_{cl} - P \preceq -Q \tag{1.9}$$

1.4 Simulation Results for System 1

By application of the second condition in proposition 1, a range of inter-sampling times h_1 has been tested to verify stability.

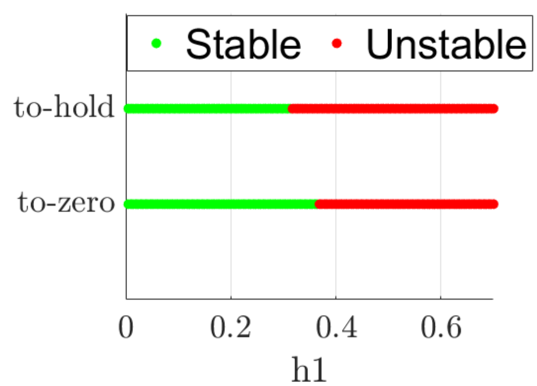

Figure 4: Comparison of system 1 stability using the to-zero or to-hold strategy as a function of inter-sampling time h_1

Using the to-zero strategy, the system is stable for a larger range of inter-sampling times than in the to-hold strategy. More precisely, it is stable up to approximately $h_1 = 0.38$ instead of $h_2 = 0.3s$. Upon comparing this with the results from assignment 1 (see figure 5) it is clear that the range of stable inter-sampling times has decreased.

[1] Note that we could also define the sequence m^1 as $(10)^\omega$ but this does not affect stability since $spec(\mathcal{F}_1^i \mathcal{F}_0) = spec(\mathcal{F}_0 \mathcal{F}_1^i)$, see theorem 1.3.22 in [2] for a proof

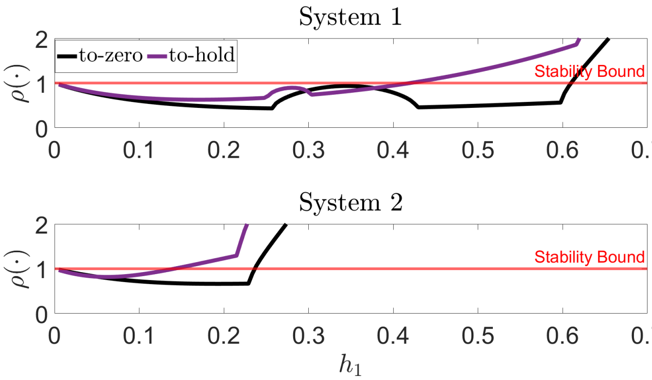

Figure 5: Stability of system 1 and system 2 using both strategies in the situation described in assignment 1 question 5

2 Probabilistic Packet Loss

2.1 Markov Chain

Figure 6 shows the Markov Chain for system 1 and system 2 jointly. Mind you, **not all transition probability maps** are shown, for the sake of overview. This is a reasonable simplification since there is a lot of symmetry in the maps, which will be explained in more detail.

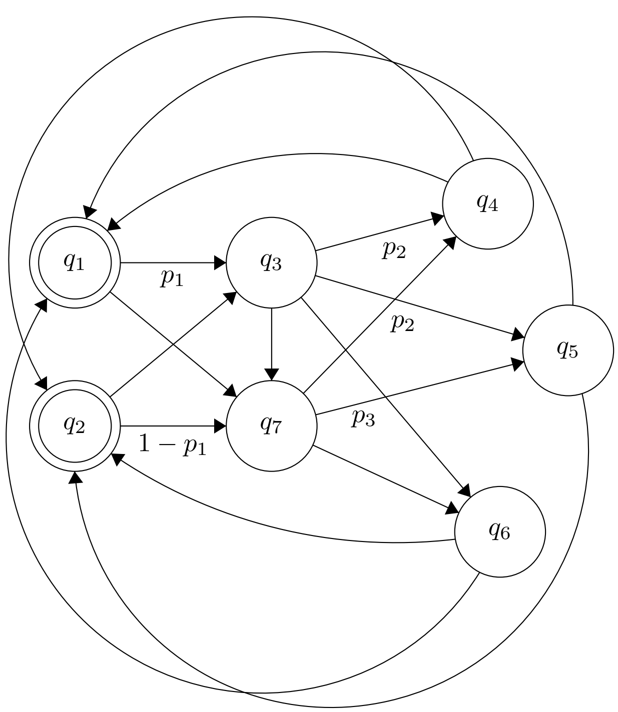

Figure 6: Markov chain of system 1 and 2 jointly

Table 1 gives an overview of what all states represent. The notation here is **R** for received and **D** for dropped packet. When for system 2 "**-**" is shown, this means that system 2 is not updated.

State	Sys 1	Sys 2
q_1	**R**	**-**
q_2	**D**	**-**
q_3	**R**	**-**
q_4	**R**	**D**
q_5	**D**	**R**
q_6	**D**	**D**
q_7	**D**	**-**

Table 1: Overview of Markov Chain states and their meaning in terms of packet drops

It can thus be seen that states q_4, q_5 and q_6 represent the sampling instants when there's a collision. Furthermore, $p_1 = 0.99$ which encapsulates the independent probability that only system 1 looses a packet when there is no collision. Lastly, $p_2 = 0.49$ and $p_3 = 0.02$, the probabilities that only 1 of both systems loses a packet at a collision and that both systems loose a packet at a collision respectively.

The transition probability matrix is given accordingly:

$$T = \begin{bmatrix} 0 & 0 & p_1 & 0 & 0 & 0 & 1-p_1 \\ 0 & 0 & p_1 & 0 & 0 & 0 & 1-p_1 \\ 0 & 0 & 0 & p_2 & p_2 & p_3 & 0 \\ p_1 & 1-p_1 & 0 & 0 & 0 & 0 & 0 \\ p_1 & 1-p_1 & 0 & 0 & 0 & 0 & 0 \\ p_1 & 1-p_1 & 0 & 0 & 0 & 0 & 0 \\ 0 & 0 & 0 & p_2 & p_2 & p_3 & 0 \end{bmatrix} \tag{2.1}$$

2.2 Markovian Jump Linear System

Let us firstly define some notation, which is very similar to the one used before. Firstly, it must be noted that the state is extended with the input at the previous sampling instant, since we're using the to-hold strategy. The extended closed dynamics of both systems are given by:

$$\begin{aligned} x^e_{k+1} &= F^{cl}_{m_k} x^e_{k+1}, \quad \text{System 1} \\ \tilde{x}^e_{k+3} &= \mathcal{F}^{cl}_{m_k} \tilde{x}^e_{k+3}, \quad \text{System 2} \end{aligned} \tag{2.2}$$

Note that $m_k = \{0, 1\}$ denotes again a packet received and lost respectively. Subsequently, we define a switching signal $r_k \in \{1, \ldots, 7\} = Q$ which represents the state in which the Markovian system is at sampling instant

k. Then, the Markovian Jump Linear System (MJLS) dynamics for the joint system are given by

$$z_{k+1} = \begin{bmatrix} x^e_{k+1} \\ \tilde{x}^e_{k+1} \end{bmatrix} = A^{cl}_{r_k} z_k \tag{2.3}$$

Where the system matrices, dependent on switching signal r_k are given by:

$$A^{cl}_1 := \begin{bmatrix} F^{cl}_0 & 0 \\ 0 & I \end{bmatrix}, \mathbb{P}(q_k = q_1 | q_{k-1} \in \{q_4, q_5, q_6\}) = p_1$$

$$A^{cl}_2 := \begin{bmatrix} F^{cl}_1 & 0 \\ 0 & I \end{bmatrix}, \mathbb{P}(q_k = q_2 | q_{k-1} \in \{q_4, q_5, q_6\}) = 1 - p_1$$

$$A^{cl}_3 := \begin{bmatrix} F^{cl}_0 & 0 \\ 0 & I \end{bmatrix}, \mathbb{P}(q_k = q_3 | q_{k-1} \in \{q_1, q_2\}) = p_1$$

$$A^{cl}_4 := \begin{bmatrix} F^{cl}_0 & 0 \\ 0 & \mathcal{F}^{cl}_1 \end{bmatrix}, \mathbb{P}(q_k = q_4 | q_{k-1} \in \{q_3, q_7\}) = p_2$$

$$A^{cl}_5 := \begin{bmatrix} F^{cl}_1 & 0 \\ 0 & \mathcal{F}^{cl}_0 \end{bmatrix}, \mathbb{P}(q_k = q_5 | q_{k-1} \in \{q_3, q_7\}) = p_2$$

$$A^{cl}_6 := \begin{bmatrix} F^{cl}_1 & 0 \\ 0 & \mathcal{F}^{cl}_1 \end{bmatrix}, \mathbb{P}(q_k = q_6 | q_{k-1} \in \{q_3, q_7\}) = p_3$$

$$A^{cl}_7 := \begin{bmatrix} F^{cl}_1 & 0 \\ 0 & I \end{bmatrix}, \mathbb{P}(q_k = q_7 | q_{k-1} \in \{q_2, q_1\}) = 1 - p_1 \tag{2.4}$$

2.3 Stochastic Stability

To analyze stochastic stability of the joint system I will use the notion of Mean Square Stability, which can be verified by the application of theorem 1

Theorem 1 *[(Costa et al., 2006), [1]] The Markovian jump linear system:*

$$z_{k+1} = A^{cl}_{r_k} z_k$$

is Mean Square Stable (MSS) if there exist $P_i \succ 0$, $i = 1, \ldots, N \in Q$*, such that:*

$$P_i - \sum_{j=1}^{N} p_{ij} (A^{cl}_j)^T P_j A^{cl}_j \succ 0, \quad \forall i = 1, \ldots, N \in Q$$

In our case, this results in solving 14 LMIs. That is, 7 LMIs for each i, which corresponds to a row in the matrix T, and 7 LMIs for each $P_i \succ 0$.

2.4 Numerical Analysis

The 14 LMIs have been solved using the `SDPT-3` solver in MATLAB in iterative fashion. Since it is necessary to employ *non*-strict inequalities, I employed an inequality with small value $\epsilon = 1E{-}3$. That is for example $P_i \succeq \epsilon I$.

Note that the verification of theorem 1 is merely a sufficient condition, hence if the LMI has no solution we can't conclude whether the system is stable or unstable. Figure 7 shows the results of the iterative analysis on a range of h_1 values, recalling that for system 2 $h_2 = 3h_1$. Upon comparing this to figure 5, it is clear that the range of h_1 values for which the system is **MSS** is much smaller than the range for which it is **GAS** with the givendeterministic dynamics. More precisely, the joint system is MSS up to $h_1 = 0.08$ whilst in assignment 1 the joint system was asymptotically stable up to $h_1 = 0.12$ in the to-hold fashion. However, one can in fact not compare the two results as they employ different LMIs due to the different nature of the problem.

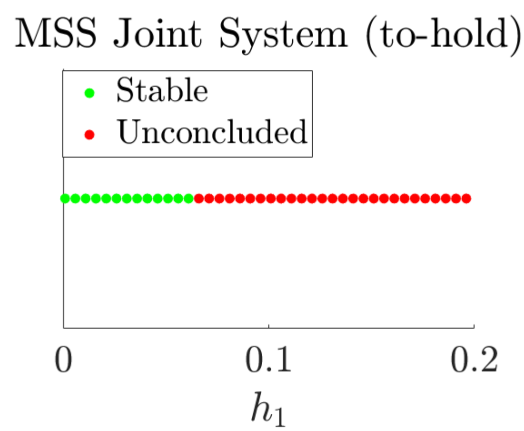

Figure 7: Range of inter-sampling times h_1 for which the joint system is MSS, concluded using an LMI analysis stated in theorem 1

3 Constant Uncertain Delay

In the remainder of this section, we ignore system 2 and consider the case where system 1 is not subject to packet-dropouts but to a constant small delay $\tau \in [0, h]$.

3.1 Polytopic Overapproximation

The uncertainty is the constant delay $\tau \in [0, h_1)$ for the inter-sampling time h_1. Therefore, by extending the state vector as $x^e_k = \begin{bmatrix} x_k & u_{k-1} \end{bmatrix}^T$, we can define the closed-loop discrete time model:

$$x_{k+1}^e = H(\tau)x_k^e \tag{3.1}$$

where H is the uncertain matrix dependent on uncertain parameter τ. That is, *a priori* uncertain but constant in the dynamics. Similar to assignment 1 define:

$$\begin{aligned} F_u(h,\tau) &= \int_{h-\tau}^{h} e^{As}B\,ds = (e^{Ah} - e^{A(h-\tau)})A^{-1}B \\ G_1(h,\tau) &= \int_{0}^{h-\tau} e^{As}B\,ds = (e^{A(h-\tau)} - I)A^{-1}B \end{aligned} \tag{3.2}$$

Then, we can define the more explicit dynamics:

$$\begin{aligned} x_{k+1}^e &:= \mathbf{F}(h,\tau)x_k^e + \mathbf{G}(h,\tau)u_k \\ \mathbf{F}(h,\tau) &:= \begin{bmatrix} F(h) & F_u(h,\tau) \\ 0 & 0 \end{bmatrix} \\ \mathbf{G}(h,\tau) &:= \begin{bmatrix} G_1(h,\tau) \\ I \end{bmatrix} \end{aligned} \tag{3.3}$$

Subsequently, we can employ the Jordan form approach to construct the polytopic discrete-time model that over-approximates the uncertain discrete-time closed-loop NCS dynamics. First, we note that the spectrum of A $spec(A) = \{-3.7, 1\} = \{\lambda_1, \lambda_2\}$. Thus, we have two distinct eigenvalue hence two Jordan blocks of size 1. The diagonalization of A is denoted as:

$$A = Q^{-1}\Lambda Q \tag{3.4}$$

Furthermore, denote the matrix exponential as

$$e^{As} = L^s$$

Such that we can rewrite:

$$\begin{aligned} F_u &= Q^{-1}\int_{h-\tau}^{h} L^s\,ds\;QB \\ G_1 &= Q^{-1}\int_{0}^{h-\tau} L^s\,ds\;QB \end{aligned} \tag{3.5}$$

Then, by defining the uncertain parameters $\alpha_1 = e^{\lambda_1(h-\tau)}$ and $\alpha_2 = e^{\lambda_2(h-\tau)}$, we can work out the integrals and define:

$$\begin{aligned} L_F^s &= \begin{bmatrix} \lambda_1^{-1}e^{\lambda_1 h} - \lambda_1^{-1}\alpha_1 & 0 \\ 0 & \lambda_2^{-1}e^{\lambda_2 h} - \lambda_2^{-1}\alpha_2 \end{bmatrix} \\ L_G^s &= \begin{bmatrix} \lambda_1^{-1}\alpha_1 - \lambda_1^{-1} & 0 \\ 0 & \lambda_2^{-1}\alpha_2 - \lambda_2^{-1} \end{bmatrix} \end{aligned} \tag{3.6}$$

Subsequently, note that since $B = \begin{bmatrix} 0 & 1 \end{bmatrix}^T$, for $Q = \begin{bmatrix} \mathbf{v}_1 & \mathbf{v}_2 \end{bmatrix}$, $QB = \mathbf{v}_2$. Thus, by factorizing:

$$\begin{aligned} L_F^s = &\underbrace{\begin{bmatrix} \lambda_1^{-1}e^{\lambda_1 h} & 0 \\ 0 & \lambda_2^{-1}e^{\lambda_2 h} \end{bmatrix}}_{F_0^s} + \underbrace{\begin{bmatrix} -\lambda_1^{-1} & 0 \\ 0 & 0 \end{bmatrix}}_{F_1^s} \\ &+ \underbrace{\begin{bmatrix} 0 & 0 \\ 0 & -\lambda_2^{-1} \end{bmatrix}}_{F_s^2} \end{aligned} \tag{3.7}$$

We can define the matrices:

$$\begin{aligned} F_0 &= \begin{bmatrix} Q^{-1}diag(e^{\lambda_1 h}, e^{\lambda_2 h})Q & Q^{-1}F_0^s\mathbf{v}_2 \\ \mathbf{0}_{1\times 2} & 0 \end{bmatrix} \\ F_1 &= \begin{bmatrix} \mathbf{0}_{2\times 2} & Q^{-1}F_1^s\mathbf{v}_2 \\ \mathbf{0}_{1\times 2} & 0 \end{bmatrix} \\ F_2 &= \begin{bmatrix} \mathbf{0}_{2\times 2} & Q^{-1}F_s^2\mathbf{v}_2 \\ \mathbf{0}_{1\times 2} & 0 \end{bmatrix} \end{aligned} \tag{3.8}$$

Such that the resulting uncertainty set in the matrix space of $\mathbf{F}(h,\tau)$:

$$\mathcal{F} = \left\{ F_0 + \sum_{i=1}^{r} \alpha_i(\tau)F_i \mid \tau \in [0, \tau_{\max}] \right\} \tag{3.9}$$

Similarly, we can factorize the other integral:

$$\begin{aligned} L_G^s = &\underbrace{\begin{bmatrix} -\lambda_1^{-1} & 0 \\ 0 & -\lambda_2^{-1} \end{bmatrix}}_{G_0^s} + \underbrace{\begin{bmatrix} \lambda_1^{-1} & 0 \\ 0 & 0 \end{bmatrix}}_{G_1^s} \\ &+ \underbrace{\begin{bmatrix} 0 & 0 \\ 0 & \lambda_2^{-1} \end{bmatrix}}_{G_s^2} \end{aligned} \tag{3.10}$$

To obtain the matrices:

$$\begin{aligned} G_0 &= \begin{bmatrix} Q^{-1}G_0^s\mathbf{v}_2 \\ 1 \end{bmatrix}, G_1 = \begin{bmatrix} Q^{-1}G_1^s\mathbf{v}_2 \\ 0 \end{bmatrix} \\ G_2 &= \begin{bmatrix} Q^{-1}G_2^s\mathbf{v}_2 \\ 0 \end{bmatrix} \end{aligned} \tag{3.11}$$

Such that the resulting uncertainty set in the matrix space of $\mathbf{G}(h,\tau)$:

$$\mathcal{G} = \left\{ G_0 + \sum_{i=1}^{r} \alpha_i(\tau)G_i \mid \tau \in [0, \tau_{\max}] \right\} \tag{3.12}$$

where $\tau_{\max} \to h$. Since τ is in a bounded but infinite set, we would have to solve infinitely many LMIs to prove stability. Therefore, we construct two sets $\overline{\mathcal{F}} \supseteq \mathcal{F}$ and $\overline{\mathcal{G}} \supseteq \mathcal{G}$, overapproximating the uncertainty sets:

$$\begin{aligned} \overline{\mathcal{F}} &= \left\{ F_0 + \sum_{i=1}^{r} \delta_i F_i \mid \delta_i \in \left[\underline{\alpha_i}, \overline{\alpha_i}\right], i = 1,2 \right\} \\ \overline{\mathcal{G}} &= \left\{ G_0 + \sum_{i=1}^{r} \delta_i G_i \mid \delta_i \in \left[\underline{\alpha_i}, \overline{\alpha_i}\right], i = 1,2 \right\} \end{aligned} \tag{3.13}$$

where $\underline{\alpha_i} = \min_\tau \alpha_i$ and $\overline{\alpha_i} = \max_\tau \alpha_i$. We can subsequently observe that these sets can be described as the *convex hull* of a finite set of vertices $co(\mathcal{H}_\mathcal{F}) = \overline{\mathcal{F}}$ and $co(\mathcal{H}_\mathcal{G}) = \overline{\mathcal{G}}$. By proving stability for the vertices we can analyze a finite instead of an infinite set of LMIs and, by convexity and linearity, conclude stability for the sets $\overline{\mathcal{F}}$ and $\overline{\mathcal{G}}$. Since $\overline{\mathcal{F}} \supseteq \mathcal{F}$ and $\overline{\mathcal{G}} \supseteq \mathcal{G}$ then we have proven stability for the uncertainty sets and we can therefore conclude whether the system is stable for the chosen range of delays.

We can define the vertices for both matrix spaces $\mathcal{H}_F = \{H_{F,1}, \dots, H_{F,N}\}$ and $\mathcal{H}_F = \{H_{G,N}, \dots, H_{G,N}\}$ with the vertices of the closed loop $\mathcal{H}_K := \{H_{K,1}, \dots, H_{K,N}\}$. Where:

$$H_{K,i} = H_{F,i} - H_{G,i} \begin{bmatrix} \overline{K} & 0 \end{bmatrix}$$

to obtain a static controller. The minimum number of vertices is 3, yielding a conservative polytopic overapproximation that includes several combinations of extreme points, not all. This is visualized in figures 8 and 9 where it can be clearly seen that due to the special structure of $\mathcal{F}$ and $\mathcal{G}$ (in the subspace of the matrix entries) a fourth vertex can be deleted.

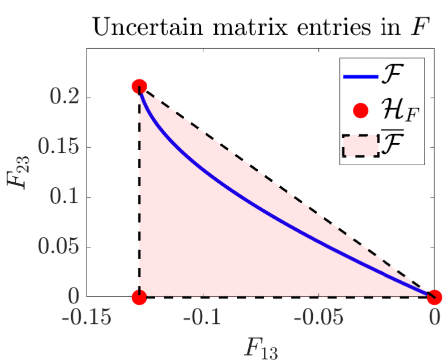

Figure 8: Visualization of the polytopic overapproximation of the uncertainty set in the matrix subspace of $\mathbf{F}$

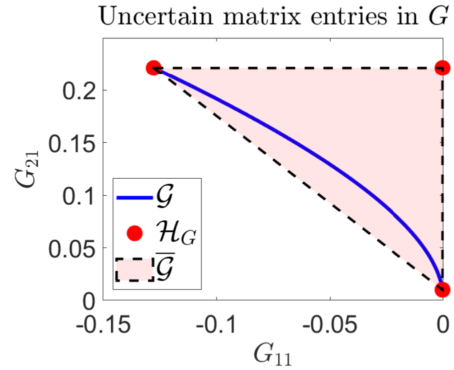

Figure 9: Visualization of the polytopic overapproximation of the uncertainty set in the matrix subspace of $\mathbf{G}$

3.2 Results: Conservative Approximation

We can guarantee *global asymptotic stability*, if there exist $P = P^T \succ 0$, $\gamma \in (0,1)$ such that the following set of LMIs is satisfied:

$$\begin{aligned} &H_{K,1}^T P H_{K,1} - P \preceq -\gamma P \\ &\vdots \\ &H_{K,3}^T P H_{K,3} - P \preceq -\gamma P \end{aligned} \tag{3.14}$$

Therefore resulting in a total of 4 LMIs. For γ, I have chosen a very small value $\gamma = 1e-5$. The reasoning behind this choice is that γ is an upper bound on the Lyapunov descent. The LMIs have been solved in MATLAB using the `SDPT3` solver. The resulting combinations for which a solution exists are given in green in figure 10 and are directly compared to the eigenvalue approach used in assignment 1.

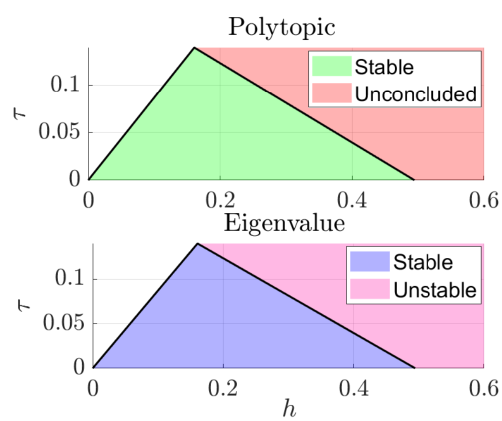

Figure 10: Comparison of stability regions using the given polytopic approximation approach (upper) and the eigenvalue approach (lower)

3.3 Results: Refined Approximation

I have employed a smaller polytope such that the approximation is less conservative. The new polytope is visualized in figures 11 and 12 in the matrix space of **F** and **G**. The newly employed polytope has a total of 4 vertices, which results in solving 5 LMIs per iteration.

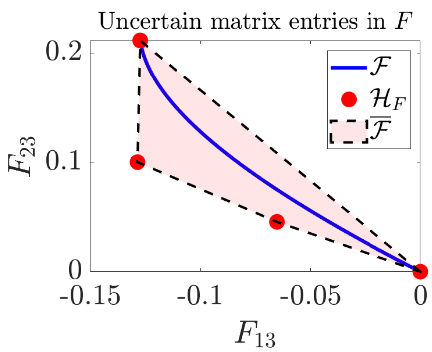

Figure 11: Visualization of the refined polytopic overapproximation of the uncertainty set in the matrix space of **F**

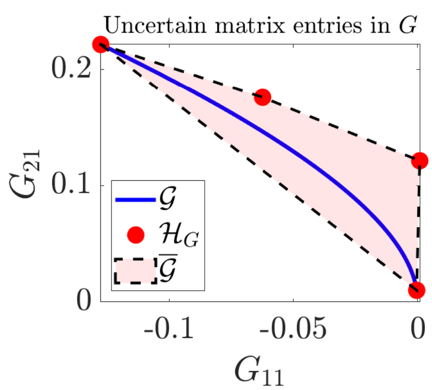

Figure 12: Visualization of the refined polytopic overapproximation of the uncertainty set in the matrix space of **G**

The new vertices have been found by scaling the uncertain parameters α_1 and α_2 through scaling of τ in the exponent, within the constraint $\tau \in [0, h)$. This has been done by trial and error, and visual inspection.

An equivalent analysis has been performed by iteratively solving the 5 LMIs:

$$\begin{aligned} &H_{K,1}^T P H_{K,1} - P \preceq -\gamma P \\ &\vdots \\ &H_{K,4}^T P H_{K,4} - P \preceq -\gamma P \\ &P \succ 0 \end{aligned} \tag{3.15}$$

The result is shown in figure 13 and directly compared to the eigenvalue analysis employed in assignment 1.

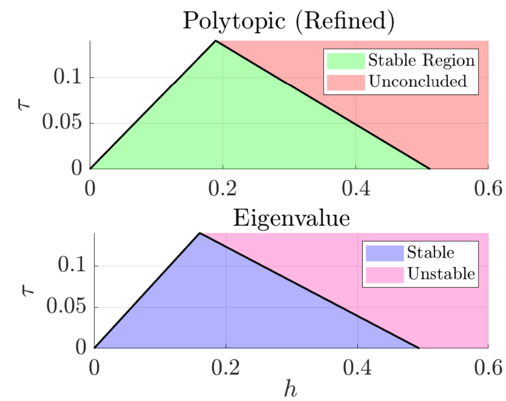

Figure 13: Comparison of stability regions using the given polytopic approximation approach with the smaller polytope (upper) and the eigenvalue approach (lower)

3.4 Discussion of Results

As is clear from the figures 8 and 9 the polytope is quite a rough approximation of the uncertainty set, in the particular matrix subspace. However, figure 10 shows (up to the analysis precision) the same stable region as in assignment 1, where an eigenvalue analysis was employed. The eigenvalue analysis provides a necessary condition on stability and is therefore less conservative. My expectation was therefore that the polytopic approach would prove stability for a smaller region due to its inherent conservatism. In that context, the result in figure 13 is not surprising since it should prove stability for at least the region provided by the larger polytope.

4 Event-Triggered Control

4.1 Event-triggering Condition

The quadratic condition chosen in this report makes use of the performance specified by the convergence rate on the Lyapunov function:

$$\frac{d}{dt}V(\xi(t)) \leq -\sigma\xi(t)^T Q\xi(t), \tag{4.1}$$

for some $\sigma \in (0,1)$. We can impose such performance making sure that for $t \in [s_k, s_{k+1}]$:

$$\begin{gathered}\phi(\xi(t),\xi(s_k)) := \begin{bmatrix}\xi(t)^T & \xi(s_k)^T\end{bmatrix} M \begin{bmatrix}\xi(t) \\ \xi(s_k)\end{bmatrix} \leq 0 \\ M := \begin{bmatrix}A^T P + PA + \sigma Q & -PBK \\ -(BK)^T P & 0\end{bmatrix}\end{gathered} \tag{4.2}$$

By increasing the σ we can impose a higher convergence rate. The system will have more "performance" in terms of exponential convergence to the origin, although the event is more easily triggered. Lastly, I choose a symmetric matrix $Q = I$.

4.2 Simulations

The system is simulated for two initial conditions and different values of σ.

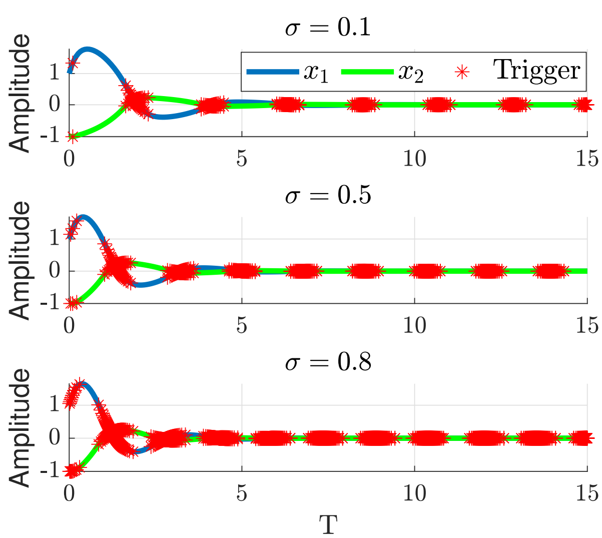

Figure 14: Simulation of ETC-system with $x_0 = \begin{bmatrix}1 & -1\end{bmatrix}^T$

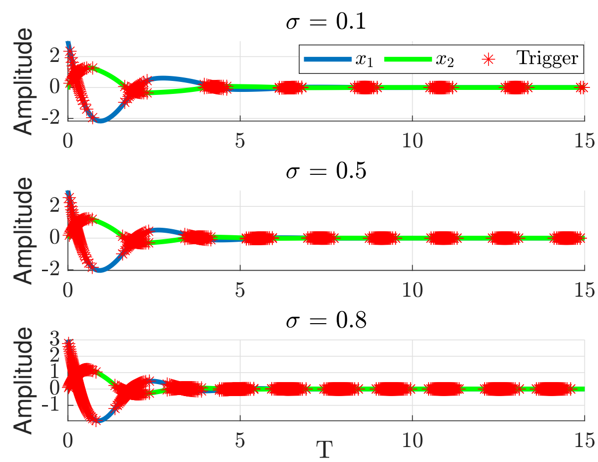

Figure 15: Simulation of ETC-system with $x_0 = \begin{bmatrix}3 & 0\end{bmatrix}^T$

In all simulations, the controller successfully stabilizes the system. Although no significant difference in the dynamics is observed due to a different σ, a pattern in event-triggering is observed. First of all, an interesting patter is visible where triggering occurs in subsequent "bursts". Secondly, it is clear that increasing the σ, corresponding to a more demanding performance specification, results in a more frequent triggering. This is an expected effect. More intuitive, if one desires more performance, it is logical to "intervene" more often.

References

[1] Oswaldo Luiz Valle Costa, Marcelo Dutra Fragoso, and Ricardo Paulino Marques. *Discrete-time Markov jump linear systems*. Springer Science & Business Media, 2006.

[2] R.A. Horn and C.R. Johnson. *Matrix Analysis*. Matrix Analysis. Cambridge University Press, 2013. ISBN: 9780521839402. URL: https://books.google.co.uk/books?id=5I5AYeeh0JUC.